Continuous-discontinuous modeling of failure in micromorphic media: localization criterion

Pamela D. N. Reges[1], Roque L. S. Pitangueira[1], Leandro L. Silva[1], Lapo Gori[1]

[1]*Dept. of Structural Engineering, Federal University of Minas Gerais*
Antônio Carlos Avenue, 6627,31270-901, Belo Horizonte/Minas Gerais, Brazil
pamelanogueira@ufmg.br, roque@dees.ufmg.br, leandro@dees.ufmg.br, lapo@dees.ufmg.br

Abstract. Deformation and failure are typically developed at multiple scales for the majority of engineering materials. At the macroscopic level of observation, structural rupture is triggered by a localized failure that corresponds to a loss in the material continuity within a specific region of the body. This localized failure is preceded by microcrack coalescence that can be observed at lower observation levels. This study investigates the propagation of a discrete fracture within a continuum damage process zone within the framework of micromorphic media. The adopted generalized continuum theory is well suited for modeling microstructured materials and also recognized in the relevant literature for its regularization properties due to its non-local formulation. Microcracking prior to coalescence is represented by continuum damage models based on a recently proposed formulation for elastic degradation in micromorphic media. The propagation of a discrete fracture aims to be based on the analysis of a generalized micromorphic acoustic tensor, which is here derived considering the concepts of acceleration waves. The required implementations for the numerical investigation of the proposed model are conducted in the open-source software INSANE aiming to determine a localization criterion for the micromorphic continuum.

Keywords: Micromorphic continuum, acoustic tensor, acceleration waves, localization analysis

1 Introduction

The constitutive modeling of a material involves describing its response to different loading conditions, characterizing its physical properties and providing the stress-strain relations. In addition, identification of the onset and description of the evolution of material failure are also required.

The failure behavior of a material is closely related to the relative size of the fracture process zone (FPZ) with respect to the structural dimensions. If the length of the process zone is comparatively small, the failure is considered brittle. Otherwise, still in the absence of plasticity, the failure is classified as quasi-brittle [1].

Considering the heterogeneity of quasi-brittle materials, models for concrete failure analysis may be divided into macroscopic and mesoscopic models [2]. Macroscopic models consider a homogeneous material, neglecting the heterogeneous composition of concrete. Depending on the crack representation, these models can be roughly classified as discontinuous or continuous. On the other hand, mesoscopic models explicitly represent the concrete heterogeneity describing its multiple phases.

A discontinuous approach considers the insertion of a displacement discontinuity into the mesh as the crack extends between elements or within an element. This discontinuity will be called hereafter a strong discontinuity, which, in physical terms, corresponds to a sharp crack [3]. In this case, the displacement field presents a jump, which can be a discontinuity curve (for a two dimensions analysis) or a discontinuity surface (for a three dimensions analysis).

Alternatively, a crack can be simulated smeared over a certain region, the localization band, in the continuous approach (or smeared crack approach). In this method the crack can be considered from a local or regularized perspective. In the first option the region of localized deformation is represented by a thin band of finite thickness. This band is separated from the rest of the body by a weak discontinuity, which can be curves or surfaces where certain strain components have a jump, but the displacement field remains continuous. In the second and most regular option the displacement and strain fields remain continuous. The high strains are spread over the band and there is a smooth transition to lower strains in the surrounding areas. Physically, this process can be viewed as a damage process zone where defects concentrate around the center [4].

The continuous and discontinuous approaches are connected as the former may be interpreted as the limited

case of the latter when the width of the localization band tends to zero [5, 6].

Besides the crack representation with either a discrete (discontinuous) or smeared crack (continuous) approach, there is also the option to combine both methods. These hybrid continuous-discontinuous strategies simulate initial micro-cracking using a continuous model, and then, when material degradation reaches a specific threshold, crack formation is simulated through the introduction of a strong discontinuity. Numerous continuous-discontinuous models have been proposed in the literature, employing different strategies for crack representation [4, 7–11].

A criterion to define where and when to insert a crack increment is essential for continuous-discontinuous strategies. Instability or loss of ellipticity, which is related to a strain localization phenomenon in quasi-brittle media, is a possible criteria for coupling the models. The study of localization can be based on the theory of acceleration waves propagation [12, 13]. This approach leads to localization conditions that rely on the spectral problem for an acoustic tensor.

Here we consider the study of the acoustic tensor as a criteria for discontinuous failure in the micromorphic continuum drawing on the theory of acceleration waves presented by [14]. The micromorphic theory [15–17], accounts for the so-called microdeformation and its gradient in addition to the macroscopic strain, being thus able to provide a mode detailed description of the material state. This generalized theory is able to model more realistically a large class of engineering materials [18–21]. The constitutive equations of the micromorphic continuum can be derived using homogenization techniques, as the one here employed proposed by [22].

In the first part of the paper, the basic expressions of the micromorphic theory are briefly recalled as well as the main expressions of micromorphic scalar-isotropic damage models. Then, the formulation for localization analysis based on acceleration waves is introduced. In the final part of the paper the results of the analysis are illustrated through a finite element simulation for a uniaxial stress state.

2 Governing equations for the micromorphic continuum

The deformation of a micromorphic elastic solid is described as a mapping from a reference placement into an actual one. In a linear approximation, the kinematics of the micromorphic continuum are determined by the displacement vector u_l and the micromotion gradient tensor ϕ_{kl}. The latter is defined as $\phi_{kl} = \chi_{kl} - \delta_{kl}$ in which χ_{kK} is the microdeformation tensor and δ_{kl} is the Kronecker delta. In this case, the following strain measures can be introduced [15, 16]

$$\epsilon_{kl} = u_{l,k} - \phi_{lk}, \qquad 2e_{kl} = \phi_{kl} + \phi_{lk}, \qquad \gamma_{klm} = \phi_{kl,m} \tag{1}$$

in which ϵ_{kl}, e_{kl}, and γ_{klm} are the linear strain tensors. In the case of isotropic linear elasticity, stress and strain measures are linked by the following constitutive equations [23]

$$t_{kl} = A_{klmn}\epsilon_{mn} + E_{klmn}e_{mn}, \quad s_{kl} = E_{mnkl}\epsilon_{mn} + B_{klmn}e_{mn}, \quad m_{klm} = C_{lmknpq}\gamma_{npq} \tag{2}$$

where t_{kl} is the stress tensor; s_{kl} is a symmetric stress tensor named micro-stress average; m_{klm} is the stress moments tensor; and A_{klmn}, B_{klmn}, C_{klmnpq}, E_{klmn} are the constitutive moduli. The construction of the constitutive equations for a linear isotropic medium demands 18 elastic parameters, in contrast to a classical isotropic continuum that only requires two parameters. To circumvent this limitation a homogenization strategy is employed as presented in [22].

2.1 Scalar-isotropic damage models

Introducing the micromorphic scalar-isotropic damage models initially requires the use of a compact tensorial representation to gather all micromorphic constitutive operators as presented in eq. (2) [24]:

$$\Sigma_{\beta\nu} = \mathcal{E}^{S}_{\beta\nu\delta\psi}\Gamma_{\delta\psi}, \text{ for } \beta, \nu, \delta, \psi = 1, 2, ...9 \tag{3}$$

where the generalized stress operator $\Sigma_{\beta\nu}$ and the generalized strain operator $\Gamma_{\delta\psi}$ represent second-order tensors with dimension nine. The generalized secant stiffness operator $\mathcal{E}^{S}{}_{\beta\nu\delta\psi}$ gathers the four constitutive operators of the micromorphic theory for isotropic linear elastic solids in a fourth-order tensor with dimension nine.

For scalar-isotropic damage models, the degrading process is characterized by the progressive reduction of the secant stiffness tensor controlled by a single scalar damage variable $\mathscr{D}$. Therefore, the total stress-strain relation can be defined as

$$\Sigma_{\beta\nu} = (1-\mathscr{D})\mathcal{E}^0{}_{\beta\nu\delta\psi}\Gamma_{\delta\psi} \tag{4}$$

wherein $\mathcal{E}^0{}_{\beta\nu\delta\psi}$ is the initial elastic operator and

$$\mathcal{E}^S_{\beta\nu\delta\psi} = (1-\mathscr{D})\mathcal{E}^0{}_{\beta\nu\delta\psi}\,. \tag{5}$$

The generalized tangent stiffness can then be written as

$$\mathcal{E}^t{}_{\beta\nu\delta\psi} = (1-\mathscr{D})\mathcal{E}^0{}_{\beta\nu\delta\psi} - \left(\frac{\partial\mathscr{D}(\Gamma_{eq})}{\partial\Gamma_{eq}}\right)\Sigma^0{}_{\beta\nu}\frac{\partial\Gamma_{eq}}{\partial\Gamma_{\delta\psi}} \tag{6}$$

where $\mathscr{D}(\Gamma_{eq})$ is a damage law that describes the evolution of the damage variable, Γ_{eq} is a generalized damage measure and $\Sigma^0{}_{\beta\nu} = \mathcal{E}^0{}_{\beta\nu\delta\psi}\Gamma_{\delta\psi}$.

For the specific case of models associated in the strain space (i.e. damage models for which the gradient of the loading function has the same direction of the degradation rule) the generalized tangent operator can be rewritten as

$$\mathcal{E}^t{}_{\beta\nu\delta\psi} = (1-\mathscr{D})\mathcal{E}^0{}_{\beta\nu\delta\psi} - \left(\frac{\partial\mathscr{D}(\Gamma_{eq})}{\partial\Gamma_{eq}}\right)\kappa\Sigma^0{}_{\beta\nu}\Sigma^0{}_{\delta\psi} \tag{7}$$

in which the parameter κ depends on the damage model. The classical associated damage models of Simo-Ju [25], Ju [26], and Marigo [27] are extended to the micromorphic continuum adopting the following damage measures [24]

$$\Gamma_{eq} = \begin{cases} \sqrt{2\psi^0} & \text{(Simo-Ju micromorphic model)} \\ \psi^0 & \text{(Ju micromorphic model)} \\ \sqrt{\frac{2\psi^0}{E}} & \text{(Marigo micromorphic model)} \end{cases} \tag{8}$$

in which $\psi^0 = \frac{1}{2}A^0{}_{klmn}\epsilon_{kl}\epsilon_{mn} + \frac{1}{2}B^0{}_{klmn}e_{kl}e_{mn} + \frac{1}{2}C^0{}_{klmnpq}\gamma_{klm}\gamma_{npq} + E^0{}_{klmn}\epsilon_{kl}e_{mn}$ and E is the material Young's modulus used to construct an equivalent micromorphic continuum through the homogenization technique.

3 Acceleration waves

An acceleration wave (or weak discontinuity) in a micromorphic medium is considered to be a singular surface on which the second spatial and second time derivatives of $\boldsymbol{u}$ and $\boldsymbol{\phi}$ have jumps, while $\boldsymbol{u}$ and $\boldsymbol{\phi}$ together with their first derivatives are continuous [14]. The wavefront moves relatively to the material with a velocity $\boldsymbol{v}$ in its normal direction $\boldsymbol{n}$. Denoting a jump of a variable a across the wavefront by double brackets ($[\![a]\!] = a^+ - a^-$), the following conditions hold

$$[\![u_i]\!] = 0, \quad [\![\phi_{ij}]\!] = 0, \quad [\![u_{i,j}]\!] = 0, \quad [\![\phi_{ij,k}]\!] = 0, \quad [\![\dot{u}_i]\!] = \left[\!\left[\frac{\partial u_i}{\partial t}\right]\!\right] = 0, \quad [\![\dot{\phi}_{ij}]\!] = \left[\!\left[\frac{\partial \phi_{ij}}{\partial t}\right]\!\right] = 0 \tag{9}$$

wherein the overdot stands for the time derivative. Equation (9) implies that the stress tensors t_{kl} and m_{klm} are also continuous across the wavefront, i.e. $[\![t_{kl}]\!] = 0$ and $[\![m_{klm}]\!] = 0$. Applying Maxwell's theorem [14] to the continuous fields results in the relations

$$[\![\dot{u}_{i,j}]\!] = a_i n_j,\ [\![\dot{\phi}_{ij,k}]\!] = A_{ij} n_k,\ [\![\ddot{u}_i]\!] = -v a_i,\ [\![\ddot{\phi}_{ij}]\!] = -v A_{ij},\ [\![t_{ik,i}]\!] = -\frac{1}{v}[\![\dot{t}_{ik}]\!] n_i,\ [\![m_{kjl,k}]\!] = -\frac{1}{v}[\![\dot{m}_{kjl}]\!] n_k \tag{10}$$

where a_i and A_{ij} are the vectorial and second-order tensorial amplitudes of the jumps.

Localization is observed when the strong ellipticity condition for the equilibrium equations for a micromorphic continuum is violated. Considering a discontinuity only in the displacement u_i ($[\![\ddot{u}_i]\!] \neq 0$ and $[\![\ddot{\phi}_{ij}]\!] = 0$), the following equation can be written

$$Q_{lp}^{t,aa} a_p = 0 \tag{11}$$

where the tangent acoustic tensor $Q_{lp}^{t,aa}$ has been introduced

$$Q_{lp}^{t,aa} = (1-D) A_{klpq}^0 n_q n_k - \frac{1}{H} t_{kl}^0 n_k \left(\kappa t_{pq}^0\right) n_q \tag{12}$$

Localization occurs when the condition defined in eq. (11) is satisfied for a normal direction $\boldsymbol{n}$, i.e., when $\det(Q_{lp}^{t,aa}) = 0$.

4 Uniaxial stress state: localization analysis

The present section is dedicated to the investigation of the behavior of the micromorphic acoustic tensor on the onset of expected localization based on the derivations presented in Section 3. The Finite Element Method (FEM) simulation has been performed with the open-source software INSANE (INteractive Structural ANalysis Environment, `http://www.insane.dees.ufmg.br`), which source code is freely available at the Git repository `https://git.insane.dees.ufmg.br/insane/insane.git`. Figure 1 illustrates the adopted model analyzed under plane stress conditions. The 3×1 m^2 panel is discretized with three 4-node quadrilateral elements with four integration points and subjected to a traction load q. The model is simulated considering both classical and micromorphic theories.

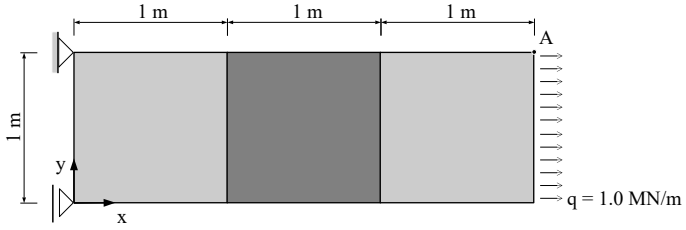

Figure 1. Uniaxial stress state: geometry

For the classical analysis, the constitutive models proposed by Simo-Ju [25], Ju [26], and Marigo [27] are employed associated to a Young's modulus $E = 20000$ MPa and a Poisson's ratio $\nu = 0.2$. For the micromorphic continuum, the generalized models presented in eq. (8) are used considering the same Young's modulus ($E = 20000$ MPa) and Poisson's ratio ($\nu = 0.2$). The adoption of the classical constants for both analysis is made possible by a homogenization technique [22] which considered, for this example, a square microcontinuum with 0.5 m to obtain the micromorphic constitutive equations.

The appropriated parameters for each constitutive model were adopted considering an exponential damage law described by, and equivalent to the classical law,

$$D(\Gamma_{eq}) = 1 - \frac{K_0}{\Gamma_{eq}}\left(1 - \alpha + \alpha e^{-\beta(\Gamma_{eq} - K_0)}\right) \tag{13}$$

in which K_0 is the threshold for the equivalent strain, and α and β define the maximum damage level allowed and the damage evolution intensity, respectively. The central element, highlighted in Fig. 1, was considered to be less resistant and associated to material M2 while the two other elements were associated to material M1. The parameters adopted for M1 and M2 considered in the classical and the micromorphic analysis are detailed in Table 1 for each damage model.

Table 1. Uniaxial stress state: constitutive parameters

Constitutive model	Parameters
Simo-Ju	M1: $\alpha = 0.999$; $\beta = 30.0$; $K_0 = 0.0148$
	M2: $\alpha = 0.999$; $\beta = 30.0$; $K_0 = 0.0133$
Ju	M1: $\alpha = 0.999$; $\beta = 15.0$; $K_0 = 0.00011$
	M2: $\alpha = 0.999$; $\beta = 15.0$; $K_0 = 0.000099$
Marigo	M1: $\alpha = 0.99$; $\beta = 4000.0$; $K_0 = 0.0001049$
	M2: $\alpha = 0.99$; $\beta = 4000.0$; $K_0 = 0.000094$

The loading process is driven by the displacement control method assuming an increment of 1×10^{-5} m for the horizontal displacement of node A (see Fig. 1), and a tolerance for the convergence of 10^{-4} in load. For the localization analysis, in order to obtain the orientation $\boldsymbol{n}$ at which the classical and micromorphic acoustic tensors becomes singular a numerical technique considering a Cartesian parametrization detailed in [28] is employed.

Figure 2 presents the results for the analysis wherein the relation between the horizontal displacement for node A (Fig. 1) and the load factor is given. Steps highlighted with an mark "X" indicate the first detection of strain localization. For the classical continuum, simulations with models Simo-Ju and Marigo displayed localization after the peak for step 29. For the Ju model, the simulation presented numerical instabilities as soon as damage initiates due to the strain localization.

The micromorphic continuum, as it can be seen in the obtained equilibrium paths illustrated in Fig. 2(b), presents some differences when compared to the classical analysis. The first observation is related to the micromorphic acoustic tensor that does not become singular as for the classical continuum. Secondly, for the micromorphic analysis the peak load is higher and the post-peak branch is not directly correlated to the exponential damage law adopted as it can be observed for the classical analysis. Lastly, there were no numerical instabilities for any of the damage models employed. These differences can be associate to the known regularization properties of generalized theories due to their non-local formulation.

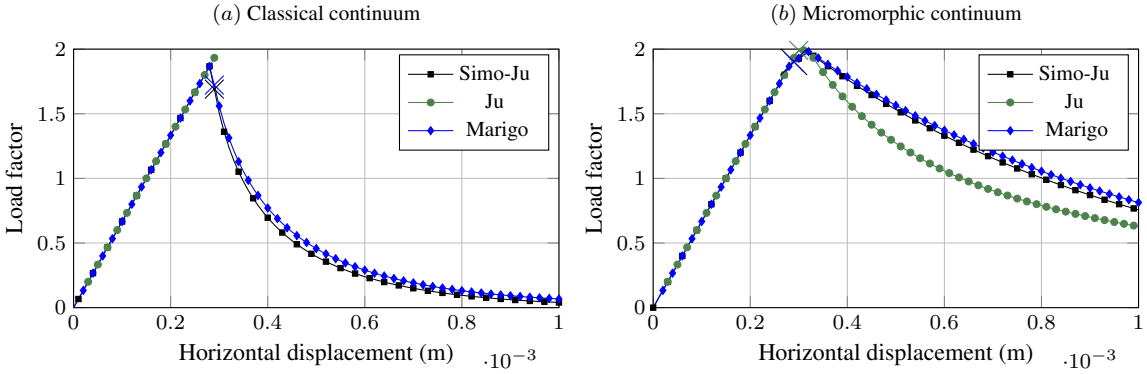

Figure 2. Uniaxial stress state: load factor versus horizontal displacement

These differences can also be observed in the damage distribution for step 100 presented in Fig. 3. For the classical continuum (Fig. 3(a)), the material degradation entirely localized in the weakened element while the others elements unloaded. The micromorphic continuum (Fig. 3(b)), on the other hand, was able to better represent this localization as, although damage concentrated in the weak element, all three elements experienced damage.

The minimum value computed for the determinant of the acoustic tensor $\boldsymbol{Q}$ at each step of both analyses is presented in Fig. 4. These results were obtained for the first integration point of the weakened element. During elastic loading, the determinant remains constant for classical and micromorphic continuum. Once damage initiates, the minimum of the determinant for the classical theory becomes negative while, for the micromorphic analysis, the determinant experience an abruptly decrease but remains positive throughout the loading process.

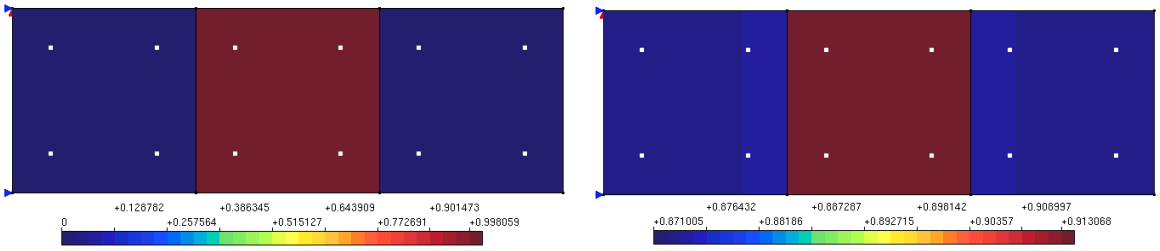

(a) Classical continuum (b) Micromorphic continuum

Figure 3. Uniaxial stress state: damage

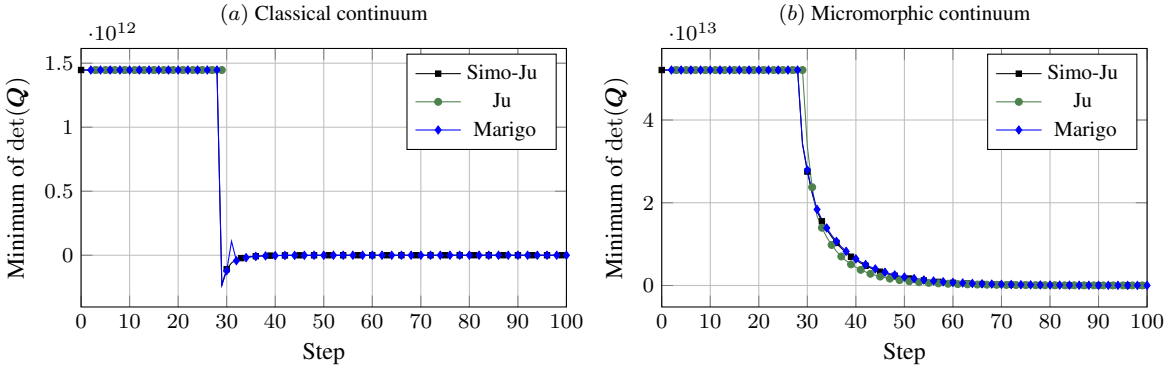

Figure 4. Uniaxial stress state: minimum of $\det(\boldsymbol{Q})$

5 Conclusions

The regularization capacity of the micromorphic theory and other generalized theories is well-know in the literature. The findings here presented attest this property through the analysis of the acoustic tensor formulated for the micromorphic theory. The results also set the path for the definition of a localization criterion that could be based on the rate of changes of the determinant of the micromorphic acoustic tensor instead of its singularity. More studies should be perform to confirm this hypotheses in order to conduct to a continuous-discontinuous model of failure that incorporate the advantages of a generalized continuum to model microstructured materials.

Acknowledgements. The authors gratefully acknowledge the support from the Brazilian research agencies CAPES (in portuguese: *Coordenação de Aperfeiçoamento de Pessoal de Nível Superior*), FAPEMIG (in portuguese: *Fundação de Amparo à Pesquisa do Estado de Minas Gerais*; grants PPM-00747-18 and APQ-01392-21), and CNPq (in portuguese: *Conselho Nacional de Desenvolvimento Científico e Tecnológico*; grant 309515/2017-3). Part of this paper was elaborated during a research stay of the second author at *Università di Trento* (financed by the *Coordenação de Aperfeiçoamento de Pessoal de Nível Superior* - CAPES - Brasil - grant 88887.910684/2023-00).

Authorship statement. The authors hereby confirm that they are the sole liable persons responsible for the authorship of this work, and that all material that has been herein included as part of the present paper is either the property (and authorship) of the authors, or has the permission of the owners to be included here.

References

[1] Z. P. Bažant and J. Planas. *Fracture and Size Effect in Concrete and Other Quasibrittle Materials*. CRC Press LLC, 1998.

[2] F. Mukhtar and A. El-Tohfa. A review on fracture propagation in concrete: Models, methods, and benchmark tests. *Engineering Fracture Mechanics*, vol. 281, pp. 109100, 2023.

[3] M. Jirásek. Modeling of localized damage and fracture in quasibrittle materials. In P. A. Vermeer, H. J. Herrmann, S. Luding, W. Ehlers, S. Diebels, and E. Ramm, eds, *Continuous and Discontinuous Modelling of Cohesive-Frictional Materials*, pp. 17–29. Springer Berlin Heidelberg, Berlin, Heidelberg, 2001.

[4] M. Jirásek and T. Zimmermann. Embedded crack model. Part II: combination with smeared cracks. *International Journal for Numerical Methods in Engineering*, vol. 50, n. 6, pp. 1291–1305, 2001a.
[5] O. Manzoli, X. Oliver, and M. Cervera. *Localización de Deformaciones: Análisis y Simulación Numérica de discontinuidades en Mecánica de Sólidos*. CIMNE, monografía CIMNE n. 44 edition, 1998.
[6] S. Saloustros, M. Cervera, and L. Pelà. Challenges, tools and applications of tracking algorithms in the numerical modelling of cracks in concrete and masonry structures. *International Scholarly Research Notices*, , n. 26, pp. 961–1005, 2019.
[7] M. Jirásek and T. Zimmermann. Embedded crack model: I. basic formulation. *International Journal for Numerical Methods in Engineering*, vol. 50, n. 6, pp. 1269–1290, 2001b.
[8] J. Oliver, A. Huespe, M. Pulido, and E. Chaves. From continuum mechanics to fracture mechanics: the strong discontinuity approach. *Engineering Fracture Mechanics*, vol. 69, n. 2, pp. 113–136, 2002.
[9] C. Comi, S. Mariani, and U. Perego. An extended fe strategy for transition from continuum damage to mode i cohesive crack propagation. *International Journal for Numerical and Analytical Methods in Geomechanics*, vol. 31, n. 2, pp. 213–238, 2007.
[10] A. Simone, G. N. Wells, and L. J. Sluys. From continuous to discontinuous failure in a gradient-enhanced continuum damage model. *Computer Methods in Applied Mechanics and Engineering*, vol. 192, n. 41, pp. 4581–4607, 2003.
[11] T. Belytschko, H. Chen, J. Xu, and G. Zi. Dynamic crack propagation based on loss of hyperbolicity and a new discontinuous enrichment. *International Journal for Numerical Methods in Engineering*, vol. 58, n. 12, pp. 1873–1905, 2003.
[12] J. Hadamard. *Leçons sur la propagation des ondes et les équations de l'hydrodynamique*. Librairie Scientifique A. Hermann, Paris, 1903.
[13] R. Hill. A general theory of uniqueness and stability in elastic-plastic solids. *Journal of the Mechanics and Physics of Solids*, vol. 6, n. 3, pp. 236–249, 1958.
[14] V. A. Eremeyev, L. P. Lebedev, and M. J. Cloud. Acceleration waves in the nonlinear micromorphic continuum. *Mechanics Research Communications*, vol. 93, pp. 70–74, 2018.
[15] A. C. Eringen and E. S. Şuhubi. Nonlinear theory of simple micro-elastic solids – i. *International Journal of Engineering Science*, vol. 2, n. 2, pp. 189–203, 1964.
[16] E. S. Şuhubi and A. C. Eringen. Nonlinear theory of simple micro-elastic solids – ii. *International Journal of Engineering Science*, vol. 2, n. 4, pp. 389–404, 1964.
[17] R. D. Mindlin. Micro-structure in linear elasticity. *Archive for Rational Mechanics and Analysis*, vol. 16, pp. 51–78. Communicated by R. A. Toupin, 1964.
[18] G. Hütter, U. Mühlich, and M. Kuna. Micromorphic homogenization of a porous medium: elastic behavior and quasi-brittle damage. *Continuum Mechanics and Thermodynamics*, vol. 27, pp. 1059–1072, 2015.
[19] R. Biswas and L. Poh. A micromorphic computational homogenization framework for heterogeneous materials. *Journal of the Mechanics and Physics of Solids*, vol. 102, pp. 187–208, 2017.
[20] J. Zhi, L. H. Poh, T.-E. Tay, and V. B. C. Tan. Direct fe2 modeling of heterogeneous materials with a micromorphic computational homogenization framework. *Computer Methods in Applied Mechanics and Engineering*, vol. 393, pp. 114837, 2022.
[21] F. Massing, S. Glane, W. H. Müller, and V. A. Eremeyev. Micromorphic theory as a model for blood in the microcirculation: correction and analysis. *Continuum Mechanics and Thermodynamics*, vol. , 2023.
[22] da L. L. Silva, da R. L. Silva Pitangueira, and S. S. Penna. Multiscale numerical strategy for micromorphic description of quasi-brittle media from classical elastic damage models at the microscale. *Applied Mathematical Modelling*, vol. 109, pp. 52–76, 2022.
[23] A. C. Eringen. *Microcontinuum Field Theories: I. Foundations and solids*. Springer, New York, 1999.
[24] P. D. Reges, R. L. Pitangueira, and L. L. Silva. Elastic degradation models for the micromorphic continuum. *International Journal of Non-Linear Mechanics*, pp. 104450, 2023.
[25] J. Simo and J. Ju. Strain- and stress-based continuum damage models–i. formulation. *International Journal of Solids and Structures*, vol. 23, n. 7, pp. 821 – 840, 1987.
[26] J. Ju. On energy-based coupled elastoplastic damage theories: Constitutive modeling and computational aspects. *Int. J. Solids Struct.*, vol. 25, n. 7, pp. 803–833, 1989.
[27] J. Marigo. Modelling of brittle and fatigue damage for elastic material by growth of microvoids. *Engineering Fracture Mechanics*, vol. 21, n. 4, pp. 861 – 874, 1985.
[28] L. A. F. Fioresi, R. L. S. Pitangueira, and S. S. Penna. Numerical technique for strain localization analysis considering a Cartesian parameterization. *Journal of the Brazilian Society of Mechanical Sciences and Engineering*, vol. 42, n. 3, pp. 145, 2020.